Journal of NeuroVirology (2000) 6, 373–381

www.jneurovirol.com

Reinvestigation of the role of the rabies virus glycoprotein in viral pathogenesis using a reverse genetics approach

Kinjiro Morimoto[1], Heather D Foley[1,3], James P McGettigan[1,3], Matthias J Schnell[2,3] and Bernhard Dietzschold*[,1]

[1]Center for Neurovirology, Department of Microbiology and Immunology, Thomas Jefferson University, 1020 Locust Street, Philadelphia, PA 19107, USA; [2]Department of Biochemistry and Molecular Pharmacology, Thomas Jefferson University, 1020 Locust Street, Philadelphia, PA 19107, USA and [3]The Dorrance H. Hamilton Laboratories, Center for Human Virology, Thomas Jefferson University, 1020 Locust Street, Philadelphia, PA 19107, USA

The rabies virus glycoprotein (G) gene of the highly neuroinvasive and neurotropic strains SHBRV-18, CVS-N2c, and CVS-B2c was introduced into the non-neuroinvasive and less neurotropic SN-10 strain to provide further insight into the role of G in the pathogenesis of rabies. Phenotypic analyses of the recombinant viruses revealed, as expected, that the neurotropism of a particular rabies virus strain was a function of its G. Nevertheless, the pathogenicity of the recombinant viruses was, in every case, markedly lower than that of the wild-type viruses suggesting that while the G dictates neurotropism, other viral attributes are also important in pathogenesis. The low pathogenicity of the recombinant viruses is at least in part due to a strong increase in transcription activity. On the other hand, the production of infectious virus by the R-SHB18 recombinant virus-infected cells was significantly delayed by comparison with SHBRV-18 wild-type virus infected-cells. Replacement of the R-SHB18 G cytoplasmic domain, transmembrane domain, and stem region with its SN-10 G counterparts neither results in a significant increase in budding efficiency nor an increase in pathogenicity. These results suggest that an optimal match of the cytoplasmic domain of G with the matrix protein may not be sufficient for maximal virus budding efficiency, which is evidently a major factor of virus pathogenicity. Our studies indicate that to maintain pathogenicity, the interactions between various structural elements of rabies virus must be highly conserved and the expression of viral proteins, in particular the G protein, must be strictly controlled. *Journal of NeuroVirology* (2000) **6,** 373–381.

Keywords: rabies virus; glycoprotein; pathogenesis; reverse genetics

Introduction

Neuroinvasiveness is the predominant characteristic of rabies virus, but the mechanisms of rabies neuropathogenesis remain unclear. The virus is usually transmitted through broken skin by bite or scratch, spreading by retrograde axonal transport and replicating exclusively in neurons with the exception of acinar cells of salivary glands (Charlton *et al*, 1979). Several studies indicate that the rabies virus glycoprotein (G) plays a crucial role in the pathogenesis of rabies. The pathogenicity of fixed rabies virus strains correlates with the presence of a determinant located in antigenic site III of G. Several virus variants with an Arg→Gln mutation at position 333 affecting antigenic site III of G completely lose their ability to kill adult immunocompetent mice (Dietzschold *et al*, 1983; Seif *et al*, 1985). On the other hand, it has been shown that some Arg→Gln variants can kill adult immunocompetent mice when infected by stereo-

*Correspondence: B Dietzschold
Received 27 March 2000; revised 25 April 2000; accepted 5 May 2000

taxic inoculation (Yang and Jackson, 1992). The reduced spread of these antigenic site III mutants within the nervous system indicates that Arg 333 of G is important for the axonal/transsynaptic spread of a lethal rabies virus infection in adult animals. However, the significance of these findings for the natural history of rabies is questionable because the mutants were obtained from highly attenuated tissue culture-adapted strains. Although most of these tissue culture-adapted strains have an intact antigenic site III, their ability to invade the nervous system from a peripheral site is far less than that of street rabies virus strains (Lawson *et al*, 1989). Thus, it appears that the pathogenic phenotype of a particular rabies virus strain is determined not only by the determinant located in antigenic site III, but also by other G determinants and probably by other viral proteins. In this context, we have recently shown that the pathogenicity of different rabies virus strains correlates with the level of G expressed on the surface of infected neurons (Morimoto *et al*, 1999). High G expression leads to apoptosis of the infected neuron and it was concluded that the axonal/transsynaptic spread of the infection is inhibited by apoptosis (Morimoto *et al*, 1999). Although pulse-chase experiments suggest that pathogenic rabies viruses regulate G expression via proteolytic degradation (Morimoto *et al*, 1999), it seems likely that the overall rate of viral RNA transcription/replication also plays a major role in determining virus pathogenicity.

In addition to regulation of viral RNA transcription and G expression, virus assembly and budding efficiency might also represent critical steps in the pathogenesis of rabies. The rabies virus matrix protein (M) plays a major role in virus budding by targeting the ribonucleoprotein complex (RNP) to the plasma membrane as well as incorporating G into the budding virions (Mebatsion *et al*, 1999). To reexamine the role of G in the pathogenesis of rabies, we introduced the coding region of the G genes from highly neuroinvasive rabies virus strains into a non-pathogenic strain and compared the properties of the rescued recombinant viruses with those of the wild-type viruses.

Results

Phenotypic characterization of rabies virus strains

Four virus strains which differ considerably from each other in both pathogenicity and neuroblastoma cell specificity (Table 1) were characterized for their neuroinvasiveness in adult mice and their ability to infect neuronal and non-neuronal cells. Two parameters relevant to the biology of rabies virus were evaluated: (1) pathogenicity index, a measure of the capacity of the virus to cause lethal disease, and (2) neuroblastoma cell specificity index, a measure of the relative susceptibility of neuroblastoma cells *versus* BHK cells. This analysis revealed that the CVS-N2c and SHBRV-18 strains were approximately 13 times and 1585 times more pathogenic, respectively, than the CVS-B2c strain, whereas the SN-10 strain was virtually non-pathogenic. However, there was no obvious correlation between pathogenicity and neuroblastoma cell specificity. For example, the neuroblastoma cell specificity index of CVS-N2c was 12.5 times higher than that of SHBRV-18, but its pathogenicity index is 126 times lower than that of SHBRV-18.

Table 1 Pathogenicity and neuroblastoma cell specificity indices of rabies virus strains

Virus strain	*Pathogenicity index*[a]	*Neuroblastoma cell specificity index*[b]
SHBRV-18	$10^{-2.7}$	$10^{1.4}$
CVS-N2c	$10^{-4.8}$	$10^{2.5}$
CVS-B2c	$10^{-5.9}$	$10^{0.7}$
SN-10	$<<10^{-8.5}$	$10^{0.1}$

[a]Pathogenicity index=log i.m. LD_{50}/ml − log virus titer/ml in NA cells, [b]Neuroblastoma cell specificity index=log virus titer/ml in NA cells − log virus titer/ml in BSR cells.

Neurotropism and pathogenicity of rabies recombinant viruses

To examine the contribution of G in determining the pathogenicity of the different rabies virus strains, recombinant viruses were generated in which the G gene of the non-pathogenic SN-10 was replaced with the G genes of CVS-B2c, CVS-N2c, and SHBRV-18 (Figure 1). Comparison of the recombinant and parental viruses for neuroblastoma cell specificity (Figure 2) showed that while SN-10 infected neuroblastoma cells and BHK cells to a similar extent, the specificity of the recombinant viruses for neuroblastoma cells was markedly increased. The neuroblastoma cell specificity indices of the recombinant viruses were similar to those of the parental viruses from which the Gs were derived. Thus, the neurotropism of a particular virus strain is largely determined by its G.

Pathogenic viruses were obtained by replacement of SN-10 G with G of CVS-N2c or CVS-B2c (Figure 3). However, the pathogenicity of the R-N2c and R-B2c recombinant viruses was 63 and 32 times lower, respectively, than that of the corresponding parental viruses CVS-N2c and CVS-B2c. Unexpectedly, the recombinant R-SHB18, which contains the G of the virus with the highest pathogenicity index, was non-pathogenic for adult mice.

In vitro *growth of recombinant viruses*

To determine whether the reduced pathogenicity of R-B2c and R-N2c, and the lack of pathogenicity of R-SHB18 might be due to reduced production of infectious virus, the time course of parental and recombinant virus production in NA cells was compared. R-N2c and R-B2c had similar rates of

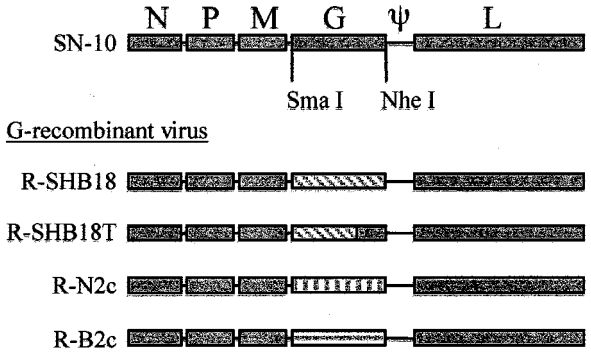

Figure 1 Schematic representation of SN-10 and recombinant rabies virus genomes. The glycoprotein (G) gene of SN-10 strain was replaced with the G genes of SHBRV-18 (diagonal stripes), CVS-N2c (vertical stripes), or CVS-B2c (horizontal stripes) strain resulting in the recombinant viruses R-SHB18, R-N2c, and R-B2c. R-SHB18T was obtained by replacing the cytoplasmic domain of its G with the corresponding amino acid sequences of SN-10 G.

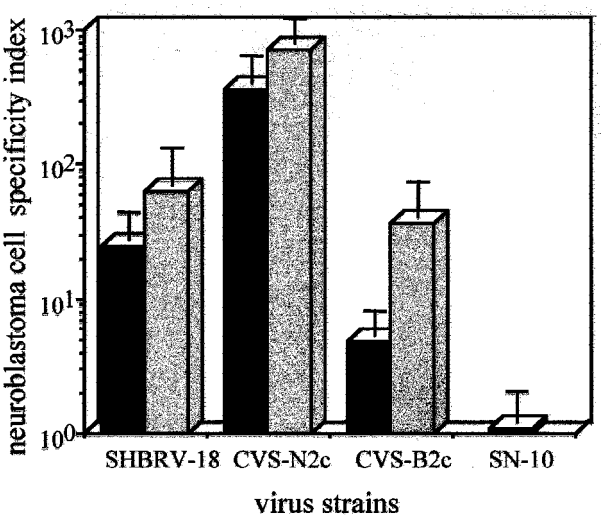

Figure 2 Neuroblastoma cell specificity index of recombinant (gray bars) and parental rabies virus stains (black bars). Neuroblastoma cell specificity index defined as log virus titer determined in mouse neuroblastoma (NA) cells minus log virus titer determined in BSR cells. Error bars indicate the standard error of the mean of six virus titer determinations.

virus production compared to the parental strains CVS-N2c, CVS-B2c, and SN-10 (Figure 4B, C). In contrast, virus titers of R-SHB18 were at 24 and 48 h p.i. 833 and 41 times lower, respectively, than those of wild-type SHBRV-18 (Figure 4A).

Viral RNA transcription and cell surface expression of recombinant virus G

To examine whether the greatly reduced replication rate of R-SHB18 corresponds with a low rate of viral transcription, the synthesis of viral N mRNA in NA cells infected with parental or recombinant viruses

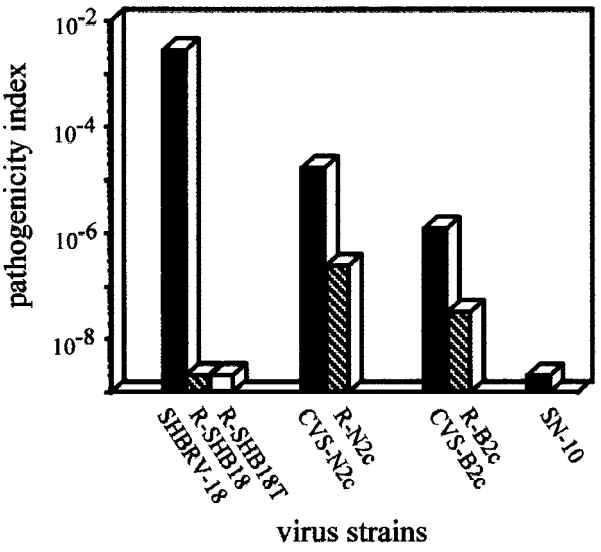

Figure 3 Pathogenicity index of recombinant and parental rabies virus strains. Pathogenicity index was defined as log intramuscular LD_{50} minus log virus titer determined in NA cells.

was compared using Northern blot analysis (Figure 5). The content of viral RNA inversely correlated with the pathogenicity index of the virus, with highest N mRNA levels observed in SN-10 infected cells (Figure 5D) and lowest levels observed in SHBRV-18-mediated cells even at 3 days after infection (Figure 5A). The content of mRNA was markedly higher in cells infected with recombinant viruses, in particular R-SHB18, compared to the corresponding wild-type strains (Figure 5E–G). Thus, the limited virus production in R-SHB18-infected cells was not due to an impairment of viral RNA transcription/replication.

Flow cytometry to measure the relative cell surface expression of each G revealed at 24 h p.i. even higher expression of G on the cell surface of R-SHB18 infected NA cells than on SHBRV-18 wild-type infected cells (Figure 6). This excludes the possibility that the reduced virus production in R-SHB18-infected cells reflected a defect in maturation and transport of G that would result in lower accumulation of G on the cell surface.

Budding efficiency and pathogenicity of recombinant viruses with a modified G cytoplasmic domain, transmembrane domain, and stem region

Interaction between the cytoplasmic domain (CD) of G and the RNP-M complex is crucial for virus budding (Mebatsion *et al*, 1999). In addition to the CD, the membrane-proximal stem region (GS) also contributes to efficient virus assembly (Robinson and Whitt, 2000). Comparison of the amino acid sequences indicates that the primary structure of the CD, the transmembrane domain (TM), and the GS of SHBRV-18 G differ markedly from those of

SN-10 G (Figure 7). The differences in the CD domains suggest a possible mismatch between the CD of SHBRV-18 G and the corresponding binding domain of the RNP-M complex of SN-10 which could, at least in part, account for the decreased budding efficiency of R-SHB18. Analysis of virus production in NA cells infected with R-SHB18T1, in which the R-SHB18 G CD was replaced with that of the SN-10 G revealed no significant increase in virus production compared to R-SHB18-infected cells at 24 and 48 h p.i. (Figure 8). Furthermore, replacement of the TM and GS domains of the R-SHB18T1 G also did not have any effect on the production of infectious virus particles (R-SHB18T2 and R-SHB18-T3, Figure 8).

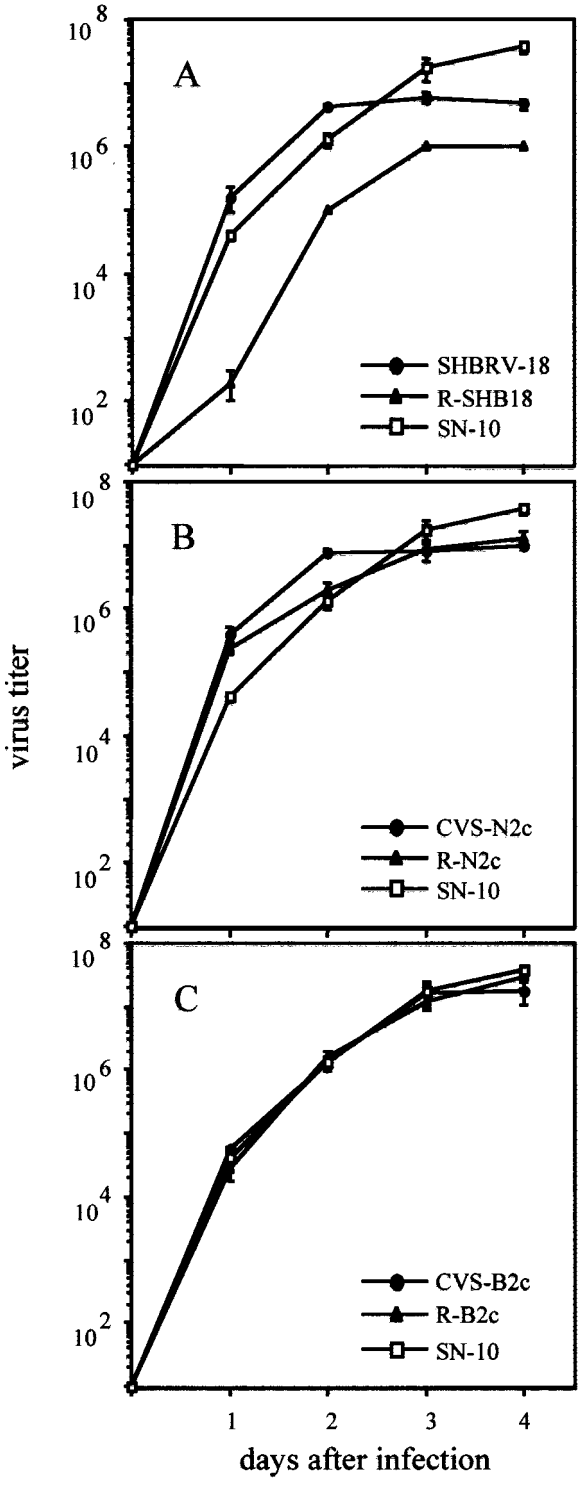

Figure 4 Rate of virus production of recombinant and parental rabies virus strains in NA cells. NA cells were infected with an m.o.i. of 1. The virus titer for m.o.i. was determined on NA cells. Viruses were harvested at days 1, 2, 3, and 4 after infection, and titrated by a fluorescent staining method. Error bars indicate the standard error of the mean of six virus titer determinations.

Discussion

Even though rabies virus has a simple genome coding for only five proteins, numerous aspects are involved in determining the pathogenicity of the virus, including regulation of transcription and replication of the viral RNA as well as differential expression of viral proteins (Morimoto *et al*, 1999; Thoulouze *et al*, 1997). Furthermore, optimal interaction of viral proteins with each other (Mebatsion *et al*, 1996a,b) and with host cell molecules that mediate internalization, replication, and egress of the virus are important in rabies pathogenesis.

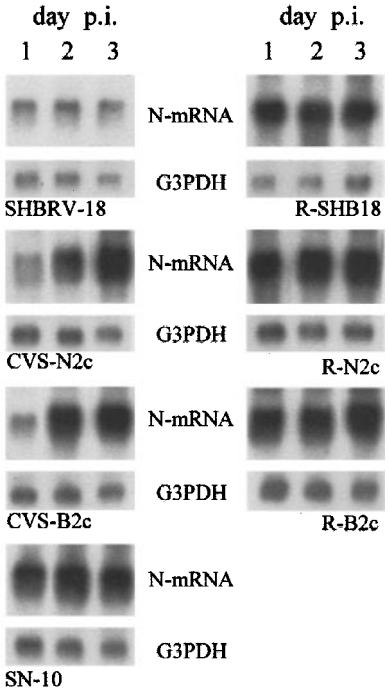

Figure 5 Production of virus mRNA. Total RNA of NA cells infected with recombinant and parental rabies viruses strains at an m.o.i. of 1 isolated at days 1, 2, and 3 after infection, electrophoresed on a 1% agarose gel, transferred to a nylon membrane, and hybridized with a probe specific for each N gene or G3PDH gene as a control.

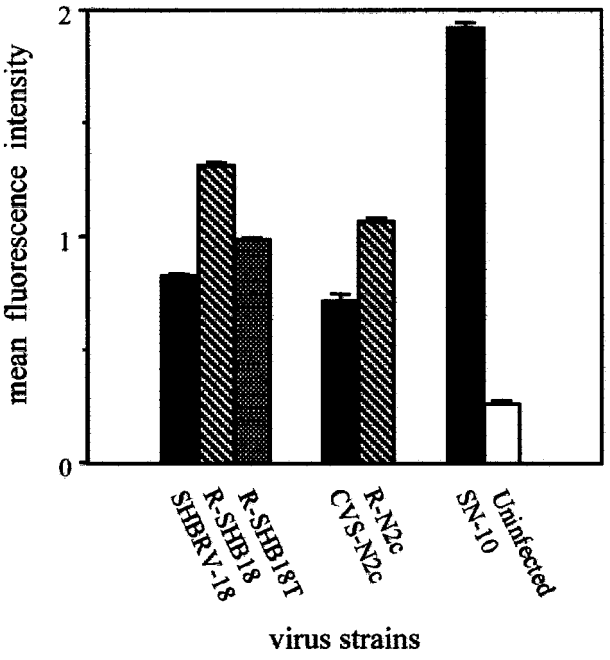

Figure 6 Cell surface expression of G. NA cells were infected with recombinant and parental rabies virus strains at an m.o.i. of 1 (determined in NA cells). At 24 h after infection, cells were removed from the dish and incubated with a rabies virus G-specific antiserum, followed by FITC-conjugated anti-rabbit antibody. Surface expression was determined by flow cytometry. Bars show the mean fluorescence intensity of the different groups of infected in non-infected cells. Error bars indicate the standard error of the mean fluorescence intensity.

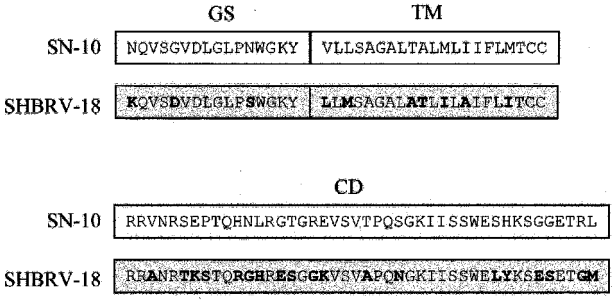

Figure 7 Amino acid sequences of the stem regions (GS), the transmembrane domains (TM), and the cytoplasmic domains (CD) of SN-10 and SHBRV-18. Amino acids different from those of SN-10 are shown in bold face.

A large body of evidence points to rabies G as a major contributor to the pathogenesis of the virus. For example, during virus uptake by the host cell, G must interact efficiently with cell surface receptors (Lentz *et al*, 1987; Thoulouze *et al*, 1998; Tuffereau *et al*, 1998) that can mediate rapid internalization of the virus. Changes in the structure of G such as an Arg→Gln exchange at position 333 significantly delay virus uptake, resulting in a marked reduction of virus spread in the CNS and complete attenuation

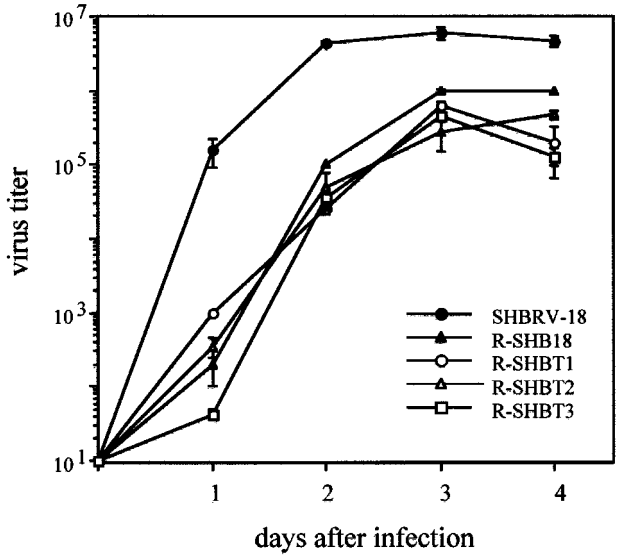

Figure 8 Effect of replacement of the CD (R-SHB18T1), the CD+TM (R-SHB18T2) and the CD+TM+GS (R-SHB18T3) on virus production. NA cells were infected at an m.o.i. of 1. Production viruses were harvested at days 1, 2, 3, and 4 after infection, and titrated by a fluorescent staining method. Error bars indicate the standard error of the mean of six virus titer determinations.

of the pathogenicity of the virus (Dietzschold *et al*, 1985; Kucera *et al*, 1985). Since rabies virus spreads primarily by the neuronal network, expression of viral proteins, especially that of G, must be strictly regulated to prevent functional impairment of the neurons due to toxicity, which would severely compromise the viral life cycle. One mechanism by which pathogenic rabies regulate G expression in neurons is proteolytic degradation (Morimoto *et al*, 1999).

To further examine the role of the rabies virus G in the pathogenesis of rabies, we exchanged the G genes of the non-neuroinvasive SN-10 strain with the G genes of neuroinvasive virus strains that differ in their pathogenicity as well as in their neurotropism. Phenotypic characterization of the resulting recombinant viruses clearly demonstrated that the ability of a rabies virus to infect neuroblastoma cells *versus* BHK cells is a function of its G. However, the pathogenicity of a rabies virus strain did not necessarily correlate with its neurotropism; only the recombinant viruses R-N2c and R-B2c, which contain the Gs of the CVS variants CVS-N2c and CVS-B2c, were pathogenic for adult mice after intramuscular inoculation. On the other hand, the R-SHB18 recombinant, which contains the G of the highly neuroinvasive SHBRV-18 strain, was completely non-pathogenic. Even in the R-N2c and R-B2c recombinants, the pathogenicity was markedly reduced as compared to that of the parental wild-type virus from which the Gs were derived, indicating that pathogenicity is not only determined

by G but also by other factors. Since the transcription levels of viral mRNA in recombinant virus-infected cells were much higher than in cells infected with pathogenic wild-type viruses, it is possible that the reduced pathogenicity observed with R-N2c and R-B2c is at least in part due to an increase in transcription activity of these viruses which could lead to apoptosis. In this context, we have recently shown that the ability of a virus strain to induce apoptosis in neuronal cells is inversely correlated with pathogenicity.

The finding that the R-SHB18 is non-pathogenic was unexpected because this recombinant virus contains the G gene of a highly neuroinvasive wild-type virus. Flow cytometry analysis demonstrated that G expression is actually greater on R-SHB18 recombinant virus-infected cells than on SHBRV-18 wild-type virus-infected cells. This data indicated intact synthesis, maturation, and transport of the R-SGB18 G. Comparison of the growth characteristics of the R-SHB18 recombinant virus and the SHBRV-18 wild-type virus revealed a significant delay in the production of infectious R-SHB18 virus particles, which could be due to a defect in virus budding arising from inefficient interaction of G with the RNP-M complex (Mebatsion *et al*, 1996a, 1999). The amino acid sequence of the SHBRV-18 G CD differs by 43% from the amino acid sequence of the SN-10 G CD and these structural differences could be responsible for this inefficient interaction. However, virus titers produced by cells infected with R-SHB18T1 containing a homologous SN-10 G CD were not significantly higher than those observed with the R-SHB18 recombinant virus, suggesting that an optimal interaction of G with M alone is not sufficient for efficient virus budding. Furthermore, virus production in cells infected with R-SHB18T3 containing homologous SN-10 GS, TM, and CD did not markedly differ from that of R-SHB18T1-infected cells. Therefore, the decreased budding efficiency of R-SHB18 most likely rests in differences in the three-dimensional structure of the G spikes of SHBRV-18 and SN-10. The amino acid sequences of the SN-10 and SHBRV-18 G ectodomains differ by 10% and these structural differences might affect the spacing of the CD of the R-SHB18T G spikes which are sterically precluded from appropriate interaction with the SN-10 RNP.

Our data support the notion that rabies virus G is a contributor to the pathogenicity of the virus. However, to invade the CNS from a peripheral site and to cause a lethal encephalitis, G must interact effectively with cell surface molecules that can mediate rapid internalization of the virus, and expression levels of G must be controlled by either regulation of viral RNA transcription or by proteolytic degradation. Finally, G must interact optimally with M and the RNP for efficient virus budding and probably also for transsynaptic spread of the virus.

The delineation of pathogenic mechanisms is relevant for the design of safe and effective live virus vaccines. Gene technology now enables controlled stepwise attenuation of the pathogenicity of a rabies virus strain by modifying the structure of the G CD, by introducing point mutations that affect antigenic site III (Arg333), and by increasing the transcription/replication activity of the virus. Reverse genetics allow the development of live attenuated rabies viruses that confer optimal protective immunity against infection with particular street rabies virus strain (e.g., raccoon rabies virus) and may represent potent vaccines for the immunization of wildlife.

Material and methods

Cells and viruses

Neuroblastoma NA cells of A/J mouse origin were grown at 37°C in RPMI 1640 medium supplemented with 10% heat-inactivated fetal bovine serum (FBS). BSR, a cloned cell line derived from BHK-21 cells, and BSR-T7, a cell line derived from BSR cells which constitutively express T7 RNA polymerase (Buchholz *et al*, 1999), were grown at 37°C in Dulbecco's modified Eagle's medium (DMEM) supplemented with 10% heat-inactivated calf serum.

CVS-N2c and CVS-B2c are subclones of the mouse-adapted CVS-24 rabies virus (Morimoto *et al*, 1998). SHBRV-18 virus is a silver-haired bat-associated street rabies virus strain isolated from a human rabies victim in the USA. This isolate was subjected to a single passage in newborn mice and a virus stock was prepared from brain tissue of these mice. SN-10 is a non-pathogenic virus strain derived from SAD B19 (Schnell *et al*, 1994).

Virus titration

To determine the virus yield, monolayers of NA or BSR cells in 96-well plates were infected with serial 10-fold dilutions of virus suspension and incubated at 34°C as described (Wiktor *et al*, 1984). At 48 h postinfection, cells were fixed in 80% acetone and stained with fluorescein isothiocyanate (FITC)-labeled rabies virus N protein-specific antibody (Centocor Inc. Malvern, PA, USA). Foci were counted using a fluorescence microscope. All titrations were carried out in triplicate.

Pathogenicity studies in mice

Groups of ten 6–8 week old Swiss Webster mice were injected in the gastrocnemius muscle with 100 μl of five- or 10-fold serial dilutions of each recombinant and the parental strain. Mice were observed for 4 weeks and the 50% lethal virus dose (LD_{50}) was calculated from the mortality rates obtained with the different virus dilutions as described (Habel, 1996).

Plasmid constructions

Recombinant rabies viruses were constructed using pSADL16 (Schnell *et al*, 1994). A *Sma*I site was introduced upstream of the G gene and a *Nhe*I site upstream of the Ψ gene by site-directed mutagenesis (GeneEditor™ Promega Inc.) using the primers RP11, 5′-CCTCAAAAGAC**CCCGGG**AAAGATGGTT CCTCAG-3′ (*Sma*I site, in bold face) and RP12, 5′-GACTGTAAGGACYG**GCTAGC**CTTTCAACGATC-CAAG-3′ (*Nhe*I site, in bold face), resulting in the plasmid pSN.

To construct recombinant virus cDNA clones containing the G gene of CVS-N2c, CVS-B2c, or SHBRV-18, a *Sma*I (or *Dra*I) and a *Nhe*I restriction site upstream and downstream, respectively, of the G gene cDNAs was introduced by PCR performed with Vent polymerase (New England BioLabs, Inc.). CVS-N2c and CVS-B2c G gene cDNAs were amplified using the forward primer CVS-Sma5, 5′-CCC**CCCG GG**AAGATGGTTCC TCAGG TTCT TTG-3′ (*Sma*I site, in bold face; start codon, underlined), and the reverse primer CVS-Nhe3, 5′-GG**GCTAGC**T-CACAGTCTGATCTCACCTC-3′ (*Nhe*I site, in bold face; stop codon, underlined). SHBRV-18 G gene cDNAs were amplified using the forward primer Bat18-Dra5, 5′-CCC**TTTAAA**AAGATGATCCCC-CAGGCTCTTCTG-3′ (*Dra*I site, in bold face; start codon, underlined) and the reverse primer Bat18-Nhe3, 5′-G G **GCTA GC**TCACA TC CC GGT CT C AC TTT-3′ (*Nhe*I site, in bold face; stop codon, underlined). The PCR products were cloned into the *Sma*I and *Nhe*I sites of pSN. The resulting plasmids were designated pR-N2c, pR-B2c and pR-SHB18.

To construct recombinant virus cDNA clones containing replaced sequences of G cytoplasmic domain, a cDNA fragment corresponding to the ectoplasmic stem region, transmembrane domain, and cytoplasmic domain of SHBRV-18 G (from start codon to *Afl*III restriction site) was ligated to a cDNA fragment corresponding to the cytoplasmic domain of SN-10 G (from *Afl*III site to stop codon), and amplified by Vent polymerase using the Bat18-Dra5 primer and RP8-Gtail3 primer, 5′-CC**TCTA-GA**TTACAGTCTGG TCTCACCCCC-3′ (*Xba*I site, in bold face; stop codon, underlined). The PCR product was cloned into the *Sma*I and *Nhe*I sites of pSN, and the resulting plasmid was designated pR-SHB18T1.

To construct recombinant virus cDNA clones containing replaced sequences of G transmembrane and cytoplasmic domain, a cDNA fragment (A fragment) corresponding to the ectoplasmic and stem region of SHBRV-18 G was amplified by using Bat18-Dra5 primer and SHB-Sal3 primer, 5′-AAG**GTCGAC**ATCCGAGACCTG-3′ (*Sal*I site, in bold face; underlined nucleotide mutated to introduce *Sal*I recognition site). A cDNA fragment (B fragment) corresponding the transmembrane and cytoplasmic domains of SN-10 G was amplified by using SN10-Sal5 primer, 5′-GGA**GTCGAC**TTGGG TCTCCCG-3′ (*Sal*I site, in bold face; underlined nucleotide mutated to introduce *Sal*I recognition site) and RP8-Gtail3 primer. A fragment (from start codon to *Sal*I restriction site) and B fragment (from *Sal*I site to stop codon) was ligated and amplified by Vent polymerase using the BAT18-Dra5 primer and RP8-Gtail3 primer. The PCR product was cloned into the *Sma*I and *Nhe*I sites of pSN, and the resulting plasmid was designated pR-SHB18T2.

To construct recombinant virus cDNA clones containing replaced sequences of G stem region, transmembrane and cytoplasmic domains, a cDNA fragment corresponding to the ectoplasmic domain of SHBRV-18 G (from start codon to *Bsp*EI restriction site) was ligated to a cDNA fragment corresponding the stem region, transmembrane and cytoplasmic domains of SN-10 G (from *Bsp*EI site to stop codon), that was amplified by using SN10-Bsp5 primer, 5′-CCT**TCCGGA**TGTGCACAATCA-3′ (*Bsp*EI site, in bold face, underlined nucleotide mutated to introduce *Bsp*EI recognition site) and RP8-Gtail3 primer, and amplified by Vent polymerase using the Bat18-Dra5 primer and RP8-Gtail3 primer. The PCR product was cloned into the *Sma*I and *Nhe*I sites of pSN, and the resulting plasmid was designated pR-SHB18T3.

Recovery of recombinant rabies viruses

Recombinant viruses were rescued as described (Buchholz *et al*, 1999; Schnell *et al*, 1994). Briefly, BSR-T7 cells were grown overnight to 80% confluency in 6-well plates in DMEM supplemented with 10% FBS. One hour before transfection, cells were washed twice with serum-free DMEM. Cells were transferred with 2.5 μg of full-length plasmid, 2.5 μg of pTIT-N, 1.25 μg of pTIT-P, 1.25 μg of pTIT-L, and 1.0 μg of pTIT-G using a $CaPO_4$ transfection kit (Stratagene, La Jolla, CA, USA). After 3 h, cells were washed twice and maintained in DMEM supplemented with 10% FBS for 3 days. The culture medium was transfected onto NA cells and incubated for 3 days at 34°C. NA cells were examined for presence of rescued virus by immunofluorescence assay with FITC-labeled rabies virus N protein-specific antibody. The supernatant of positive cell cultures was injected into suckling mouse brain, and 3–4 days later, brains were removed and prepared as a 20% suspension in phosphate-buffered saline (PBS) for virus stock in further experiments. Rescued viruses generated from full-length plasmids; pR-N2c, pR-B2c, pR-SHB18, pR-SHB18T1, pR-SHB18T2, and pR-SHB18T3 were designated R-N2c, R-B2c, R-SHB18, R-SHB18T1, R-SHB18T2, and R-SHB18T3, respectively. Sequences of recombinant viruses were confirmed by sequencing of RT–PCR fragments.

RNA extraction and Northern blot analysis

Total RNA was isolated from NA cells at days 1, 2, and 3 after infection using the RNAzol B method

(Biotex Laboratories, Inc., Houston, TX, USA) according to the manufacturer's instruction. Five μg of RNA were electrophoresed on a 1% agarose gel containing 2.2 M formaldehyde and 0.1 M MOPS buffer (pH 7.0), blotted on Nytran nylon membrane, and hybridized with a nick-translated [α-^{32}P]dCTP-labeled probe. PCR products of the N gene of CVS-N2c, CVS-B2c, SHBRV-18, and SN-10 were separately prepared by amplification using the primer set N5-a (5′-ATGGATGCCGACAAGATT-3′) and N589-3 (5′-TACTCCAATTAGCACACAT-3′). As an internal control, the PCR product of glyceraldehyde-3-phosphate dehydrogenase (G3PDH) (sense primer, 5′-TGCCAAGGCTGTGGGCAAGGTCAT-3′; antisense primer, 5′-GGCCATGAGGTCCACCACCC TGTT-3′) was used.

Flow cytometry

NA cells were infected with recombinant rabies viruses or parental strains at an m.o.i. of 1 and incubated for 24 h at 34°C. Cells were suspended in PBS containing 50 mM EDTA, pelleted at 130 × g for 5 min, resuspended in 50 μl of PBS, and fixed in suspension by addition of 500 μl of 4% paraformaldehyde solution. After 20 min, the cells were washed twice with PBS containing 10 mM glycine and 1% BSA (PBS-glycine-BSA), and incubated with rabbit anti-rabies G-specific antiserum (1 : 400) followed by FITC-conjugated affinity-purified goat anti-rabbit antibody (1 : 200). Flow cytometry was performed on an EPICS profile analyzer. Error bars indicate the standard error of the mean fluorescence intensity.

Acknowledgements

We thank Suchita Santosh Hodawadekar for excellent tecPhnical help. This work was supported by Public Health Service grants AI 45097 and AI 41544.

References

Buchholz UJ, Finke S, Conzelmann K-K (1999). Generation of bovine respiratory syncytial virus (BRSV) from cDNA: BRSV NS2 is not essential for virus replication in tissue culture, and the human RSV leader region acts as a functional BSRV genome promoter. *J Virol* **73:** 251–259.

Charlton KM, Casey GA (1979). Experimental rabies in skunks: Immunofluorescent, light and electron microscopic studies. *Lab Invest* **41:** 36–44.

Dietzschold B, Wunner WH, Wiktor TJ, Lopes AS, Lafon M, Smith CL, Koprowski H (1983). Characterization of an antigenic determinant of the glycoprotein that correlates with pathogenicity of rabies virus. *Proc Natl Acad Sci USA* **80:** 70–74.

Dietzschold B, Wiktor TK, Trojanowski JQ, Macfarlan RI, Wunner WH, Torres-Anjel MJ, Koprowski H (1985). Differences in cell-to-cell spread of pathogenic and apathogenic rabies virus in vivo and in vitro. *J Virol* **56:** 12–18.

Habel K (1996). In *Laboratory Techniques in Rabies*. World Health Organization, Geneva, Monograph Series No. 23, pp. 321–335.

Kucera P, Dolivo M, Coulon P, Flamand A (1985). Pathways of the early propagation of virulent and avirulent rabies strains from the eye to the brain. *J Virol* **55:** 158–162.

Lawson KF, Hertler R, Charlton KM, Campbell JB, Rhodes AJ (1989). Safety and immunogenicity of ERA strains of rabies virus propagated in a BHK-21 cell line. *Can J Vet Res* **53:** 438–444.

Lentz TL, Hawrot E, Wilson PT (1987). Synthetic peptides corresponding to sequences of snake venom neurotoxins and rabies virus glycoprotein bind to the nicotinic acetylcholine receptor. *Proteins Struct Funct Genet* **2:** 298–307.

Mebatsion T, Conzelmann K-K (1996a). Specific infection of CD4$^+$ target cells by recombinant rabies virus pseudotypes carrying the HIV-1 envelope spike protein. *Proc Natl Acad Sci USA* **93:** 11366–11370.

Mebatsion T, Konig M, Conzelmann K-K (1996b). Budding of rabies virus particles in the absence of the spike glycoprotein. *Cell* **84:** 941–951.

Mebatsion T, Weiland F, Conzelmann K-K (1999). Matrix protein of rabies virus is responsible for the assembly and budding of bullet-shaped particles and interacts with the transmembrane spike glycoprotein G. *J Virol* **73:** 242–250.

Morimoto K, Hooper DC, Carbaugh H, Fu ZF, Koprowski H, Dietzschold B (1998). Rabies virus quasispecies: Implications for pathogenesis. *Proc Natl Acad Sci USA* **95:** 3152–3156.

Morimoto K, Hooper DC, Spitsin S, Koprowski H, Dietzschold B (1999). Pathogenicity of different rabies virus variants inversely correlates with apoptosis and rabies virus glycoprotein expression in infected primary neuron cultures. *J Virol* **73:** 510–518.

Robinson CS, Whitt MA (2000). The membrane-proximal stem region of vesicular stomatitis virus G confers efficient virus assembly. *J Virol* **74:** 2239–2246.

Schnell MJ, Mebatsion T, Conzelmann K-K (1994). Infectious rabies virus from cloned cDNA. *EMBO J* **13:** 4195–4203.

Seif I, Coulon P, Rollin PE, Flamand A (1985). Rabies virulence: effect on pathogenicity and sequence characterization of rabies virus mutations affecting antigenic site III of the glycoprotein. *J Virol* **53:** 926–934.

Thoulouze M-I, Lafage M, Montano-Hirose JA, Lafon M (1997). Rabies virus infects mouse and human lymphocytes and induces apoptosis. *J Virol* **71:** 7372–7380.

Thoulouze M-I, Lafage M, Schachner M, Hartmann U, Cremer H, Lafon M (1998). The neural cell adhesion molecule is a receptor for rabies virus. *J Virol* **72:** 7181–7190.

Tuffereau C, Benejean J, Blondel D, Kieffer B, Flammand A (1998). Low-affinity nerve-growth factor receptor (P75NTR) can serve as a receptor for rabies virus. *EMBO J* **17:** 7250–7259.

Wiktor TJ, MacFarlan RI, Foggin CM, Koprowski H (1984). Antigenic analysis of rabies and Mokola virus from Zimbabwe using monoclonal antibodies. *Dev Biol Stand* **57:** 199–221.

Yang C, Jackson AL (1992). Basis of neurovirulent rabies virus variant AvO1 with stereotaxic brain inoculation in mice. *J Gen Virol* **73:** 895–900.